



# CHORUS

This is the accepted manuscript made available via CHORUS. The article has been published as:

## Wetting of a Multiarm Star-Shaped Molecule

Emmanouil Glynos, Bradley Frieberg, and Peter F. Green

Phys. Rev. Lett. **107**, 118303 — Published 9 September 2011

DOI: [10.1103/PhysRevLett.107.118303](https://doi.org/10.1103/PhysRevLett.107.118303)

## **Wetting of a Multi-arm Star-shaped Molecule**

Emmanouil Glynos<sup>1</sup>, Bradley Frieberg<sup>2</sup>, and Peter F. Green<sup>1</sup>

<sup>1</sup>Department of materials Science and Engineering, <sup>2</sup>Macromolecular Science and Engineering University of Michigan, Ann Arbor, Michigan 48109 USA

### **Abstract**

**The equilibrium contact angles and line tensions of macroscopic droplets, composed of star-shaped polystyrene macromolecules, on silicon oxide substrates, are shown to be smaller than their linear analogs by approximately one and two orders of magnitude, respectively. A precursor layer, of lateral dimensions and of thicknesses on the order of nanometers, surrounds each droplet of low molecular weight linear PS chains. Droplets composed of star-shaped molecules possessing a sufficient number of arms, reside on a layer adsorbed to the substrate.**

The topic of wetting continues to garner much interest for reasons that include the fact that reliable strategies now exist to fabricate patterned surfaces possessing wetting properties, tailored through surface chemistry and, or, topography, at the nano-scale. Moreover the use of atomic force microscopy (AFM), and other techniques, capable of imaging the structure of liquids at the nano-scale makes it possible to carefully examine the role of short-range and long-range intermolecular forces on the structure and dynamics of liquids on surfaces.[1-7]

The dimensions of droplets on a surface may be readily controlled, experimentally, by inducing thin films, possessing specific thicknesses to dewet. The free energy per unit area of a film of nanoscale thickness,  $h$ , is determined by a combination of short- and long-range intermolecular forces, embodied in an effective interface potential,  $\phi(h)$ , defined as the excess free energy per unit area of a film of thickness  $h$ . [4]: . When the curvature,  $\Pi(h)=d\phi(h)/dh$ , of the interface potential is negative the film is unstable and breaks up via a ‘spontaneous’ spinodal mechanism, otherwise it could be stable or metastable, wherein the destabilization occurs via a nucleation and growth process.

Intermolecular forces are generally known to be responsible for the dewetting of thin polystyrene (PS) films from oxidized silicon substrates ( $\text{SiO}_x$ ), resulting in the formation of droplets, characterized by macroscopic contact angles; these droplets are surrounded by a dense collection of considerably smaller droplets of nano-scale dimensions (“nano-droplets”) [8-10]. The nano-droplets are believed to be remnants of a very thin wetting layer, whose formation, and thickness, is implied by the shape (a minimum) in the interface potential. While the driving force for their formation is suggested to be entropic in origin, it remains an open question. Further insight into

fundamental issues regarding the role of entropy on the wetting of macromolecules may be gained by considering branched molecules.

Theory and simulations reveal that star-shaped molecules are known to suffer a much smaller entropic loss when adsorbed onto substrates [11-13] and they possess lower surface energy, than their linear analogs of the same degree of polymerization,  $N$ . [14, 15] We show that star-shaped polymers possess considerably lower contact angles and line tensions than their linear analogs. Unlike linear chains, star-shaped polymers of sufficiently high functionality,  $f$ , exhibit evidence of structuring at a substrate, stable (or metastable) wetting layer formation, due evidently to entropic effects.

Thin films of a series of linear and star-shaped polystyrene (PS) molecules possessing different functionalities (3-, 4-, and 8-arms) and different molecular weights were prepared. The films were annealed at 160° C in vacuum until dewetting, droplet formation, was complete, then probed using tapping-mode AFM (for more details on the molecular characteristics of the polymer used in this study, sample preparation and AFM measurements see Supplementary Material). The morphologies of the linear chain PS, PS( $M_w = 5$  kg/mol), and the star-shaped PS, (8 arms and  $M_w$  per arm  $M_w^{\text{arm}} = 10$  g/mol) films of thickness  $h \sim 13$  nm, at the final stage of dewetting are shown in FIG 1a and 1c, respectively. A detailed assessment of the AFM images of a destabilized linear PS film reveals the existence of two collections of droplets: macroscopic droplets, as shown in FIG 1a, surrounded by nano-droplets. [10]., These nano-droplets are the result of the break-up of the wetting layer (mesolayer that). The thin layer at the periphery of the droplet, FIG 1b, the precursor layer, is a remnant of the mesolayer layer.

The behavior of the 3- and 4-arm star molecules ( $M_w^{\text{arm}}=19\text{kg/mol.}$  and  $4\text{kg/mol.}$ , respectively) is similar to the linear chains; the mesolayer broke up into nanodroplets (Figure S1 in Supplementary Material). Calculations of the total volume per unit area of the nano-droplets indicate that the thickness of the mesolayer would have been  $h_L \sim 0.27$  nm for the linear PS,  $h_S^{3\text{-arm}} \sim 0.31$  nm for the 3-arm star and  $h_S^{4\text{-arm}} \sim 0.72$  nm for the 4-arm star PS. The linear PS mesolayer thickness, based on its  $M_w$ , is in a good agreement with the reported values [9, 10, 16]. Microscopically, the conformation of a single linear chain in a melt, weakly adsorbed onto a surface, is determined by the competition between a gain in adsorption energy, due to monomers in contact with the substrate, and an entropic “repulsion” due to the loss of conformational entropy of the chain.[17] That the thickness of the mesolayer was  $h_L \sim 0.3$  nm (i.e.: thickness of the order of the monomer size) indicates that the adsorbed polymer chains are laterally extended at the substrate, maximizing their gain in adsorption energy.

In contrast, the 8-arm star PS film broke up forming a dense collection of macroscopic droplets (FIG 1c), residing on a mesolayer layer of polymer of thickness 7.8 nm. The image in FIG 2a is a cross section of the edge of a film of initial thickness  $h=30$  nm, which dewets leaving a uniform layer of thickness  $h_S^{8\text{-arm}}=7.8$  nm (FIG 2a, inset), after scratching and annealing 12h at  $160^\circ\text{C}$ . This layer is stable and in fact the temperature dependence of its thickness, measured using in situ AFM, is plotted in FIG 2b. The kink in the plot at a temperature  $T=103^\circ\text{C}$  is evidence of a glass transition temperature,  $T_g$ , which is 25 degrees higher than the bulk  $T_g$ . It is consistent with prior measurements of the thickness dependence of  $T_g$  of thin films of this polymer, in a larger

thickness range[18]. The important point is that the film is strongly adsorbed to the substrate.

The contact angle,  $\theta$ , of the macroscopic droplets at the final stage of dewetting may be determined using the relation  $\tan(\theta/2) = H/R_D$ , where  $H$  is the height and  $R_D$  the radius of the droplet. [19].  $\theta$  is shown to decrease with increasing  $R_D$  for all systems, FIG. 3, though the dependence gradually become weaker as the functionality of the molecule increased; the slope is - 0.84 degrees/ $\mu\text{m}$  and -0.89 degrees/ $\mu\text{m}$  for the linear ( $f=2$ ) and the 3-arm star respectively. The slope is -0.67 degrees/ $\mu\text{m}$  for  $f=4$ , and - 0.26 degrees/ $\mu\text{m}$  for  $f=8$ . Furthermore, the extrapolated contact angles, for infinitely large droplet composed of linear molecules are similar with the 3-arm star ( $\theta^*(\text{linear}) = 21.72 \pm 1^\circ$ , and  $\theta^*(3\text{-arm}) = 20.5 \pm 0.8^\circ$ , respectively). In the case of the 4-arm star the angle decreased to  $\theta^*(4\text{-arm}) = 15.2 \pm 0.3^\circ$ , whereas for the 8-arm molecule the angle is nearly an order of magnitude smaller:  $\theta^*(8\text{-star}) = 2.52^\circ \pm 0.1$ . Clearly there is a systematic trend, decreasing  $\theta^*$  and slope, with increasing functionality of the molecule.

We now consider consequences of the effective interface on the structure of the system, particularly with regard to the adsorbed layers. For the system of interest in this study, the effective interface potential may be written as[10]:

$$\phi_L(h_{eq}^L) = -\frac{A_{\text{air-PS-SiO}_2}}{12\pi h_{eq}^2} - \frac{A_{\text{air-PS-Si}} - A_{\text{air-PS-SiO}_2}}{12\pi(h_{eq} + d_{ox})^2} + \frac{\beta}{h^8} \quad 1.$$

where  $d_{ox}$  is the thickness of the oxidized layer;  $A_{\text{air-PS-SiO}_2}$  and  $A_{\text{air-PS-Si}}$  are the Hamaker constants of the air/PS/SiO<sub>2</sub> and air/PS/Si systems, respectively:  $A_{\text{air-PS-SiO}_2} = 2.93 \times 10^{-20}$  J and  $A_{\text{air-PS-Si}} = -4.87 \times 10^{-20}$  J. The first two terms in this relation are the classical

unretarded van der Waals forces between the media PS, SiO<sub>x</sub>, Si; the third term,  $\beta$ , represents the strength of the sort-range forces. The short-range contribution is estimated by taking advantage of a relation between the measured contact angle of an infinite size droplet and the global minimum of the effective interfacial potential. The minimum of the interface potential is related to the contact angle  $\theta$  via  $\phi_{\min} = \gamma_{LV}(\cos \theta - 1)$ [16].

We now discuss the surface tension of star-shaped polymers and compare it to the linear chain system. Lattice theory predicts that the surface tension of a star-shaped

polymer maybe reasonably represented by  $\gamma^S(M_n) - \gamma^S(\infty) = \rho RT \frac{(fU^e + U^b)}{M_n^S}$  [15],

where  $M_n$  is the average number molecular weight,  $\gamma(\infty)$  is the surface tension at the infinite  $M_n$ ,  $\rho$  is the bulk density,  $R$  is the universal gas constant (8.314 J K<sup>-1</sup>mol<sup>-1</sup>),  $T$  is the temperature, and  $U^e$  and  $U^b$  represents the effective attractive, or repulsive, interactions between the interface and the chain ends and branch point, respectively.

Minikanti and Archer, using self-consistent field theory, estimated that  $\rho RT(fU^e + U^b) = -5.4 \text{ mJ}\cdot\text{Kg/m}^2\cdot\text{mol}$ ,  $-6.6 \text{ mJ}\cdot\text{Kg/m}^2\cdot\text{mol}$ . And  $-14.5 \text{ mJ}\cdot\text{Kg/m}^2\cdot\text{mol}$ , for the 3-arm, 4-arm and 8-arm molecules, respectively. [15, 20].  $\gamma^L(\infty)$  was estimated experimentally measured values for the surface tension of linear PS melts at different molecular weights and temperatures at 160 °C  $\gamma^L(\infty) = 30.8 \text{ mJ/m}^2$ [21].  $\rho$  is taken to be the mass density of an infinite molecular weight PS at 160 °C, 989 kg/m<sup>3</sup> [22].

We determined the surface tensions of the star PS molecules, using the above procedure, to be  $\gamma^{S3\text{-arm}} = 30.5 \text{ mJ/m}^2$ ,  $\gamma^{S4\text{-arm}} = 29.1 \text{ mJ/m}^2$  and  $\gamma^{S8\text{-arm}} = 29.3 \text{ mJ/m}^2$  for the 3-arm, 4-arm and 8-arm molecules, respectively. The surface tension of the linear PS

used in this study is, at  $T=160\text{ }^{\circ}\text{C}$ ,  $\gamma^L=30.1\text{ mJ/m}^2$  [21]. The line tension was readily determined using  $\cos(\theta(R_D)) = \cos(\theta^*) - \Gamma/(\gamma_{LV}R)$  [19]. Based on the surface tension of the linear and the star-shaped molecules and the  $\cos\theta_e$  vs.  $1/R_D$  data, it follows that the line tensions of the polymers were:  $\Gamma(\text{linear})=2.61 \times 10^{-10}\text{ J/m}$ ,  $\Gamma(\text{3-arm})=2.95 \times 10^{-10}\text{ J/m}$ ,  $\Gamma(\text{4-arm})=4.94 \times 10^{-11}\text{ J/m}$ , and  $\Gamma(\text{8-arm})=7.08 \times 10^{-12}\text{ J/m}$ . Clearly, the line tension decreased with increasing functionality; it is two orders of magnitude smaller for the 8-arm star-shaped molecule than the linear chains.

We estimated the minimum of the interface potential (eq. 1) for each polymer, based on knowledge of the contact angles. For the linear chain system,  $\phi_{\min}^L = -2.14\text{ mJ/m}^2$ ,  $\phi_{\min}^{S3} = -1.93\text{ mJ/m}^2$  for the 3-arms,  $\phi_{\min}^{S4} = -5.31 \times 10^{-1}\text{ mJ/m}^2$  for the 4-arms, and  $\phi_{\min}^{S8} = -2.84 \times 10^{-2}\text{ mJ/m}^2$  for the 8-arm, star-shaped molecules. These results indicate that the spreading coefficients of the 4-arm star and the 8-arm molecules are one and two orders of magnitude smaller than that of the linear chain.

We moreover determined the strength of the short-range attractions by adjusting the parameter  $\beta$  until the depth of the minimum in the effective interface potential matched the experimentally measured values, based on the contact angles. The values were  $\beta^L = 1.88 \times 10^{-78}\text{ J m}^6$  for the linear PS, and  $\beta^{S3} = 2.42 \times 10^{-78}\text{ J m}^6$ ,  $\beta^{S4} = 4.29 \times 10^{-77}\text{ J m}^6$ , and  $\beta^{S8} = 1.95 \times 10^{-75}\text{ J m}^6$  for the star-shaped molecules possessing 3-, 4- and 8-arms, respectively. The magnitude of  $\beta$  is connected to the position of the global minimum which for the linear PS is  $h_{\min}(\text{linear}) \approx 0.4\text{ nm}$ ,  $h_{\min}(\text{3-arms}) \approx 0.45\text{ nm}$ ,  $h_{\min}(\text{4-arms}) \approx 0.8\text{ nm}$ , and  $h_{\min}(\text{8-arms}) \approx 1.6\text{ nm}$  for the 3-, 4-, and 8- arm molecules,

respectively. These minima should, in principle, correspond to the thickness of the experimentally measured mesolayers  $h_L$ ,  $h_S^{3\text{-arm}}$ ,  $h_S^{4\text{-arm}}$ , and  $h_S^{8\text{-arm}}$ .

The locations of the minima of the effective interface potentials for the linear chain the 3- and 4- arm star chain system is consistent with the mesolayer thickness of these systems. We note that the mesolayer thickness for the 4-arm was approximately twice as large as that of the linear PS and the 3-arm star PS. This observation is rationalized in terms of the differences between the adsorption behavior and of star-shaped and linear macromolecules at interfaces, which is especially important when the functionality of the star polymer increases. The 4-arm star is expected to have stronger entropic attraction with the substrate; the strength of the parameter  $\beta$ , an order of magnitude smaller than that of the linear and the 3-arm star, corroborates this assessment.

We now discuss the apparently surprising thickness of the layer formed by the 8-arm star-shaped molecules  $h_S^{\text{arm}}=7.8$  nm. The radius of gyration of a star-shaped polymer is given by  $\langle R_g^2 \rangle_{\text{star}} \sim \frac{3f-2}{f^2} \langle R_g^2 \rangle_{\text{linear}}$ , where  $f$  is the functionality of the star-shaped polymer and  $\langle R_g^2 \rangle_{\text{linear}}$  is defined as the mean-square radius of gyration of a linear chain of equal degree of polymerization with the star.[23] Using coarse-grained bead-spring models and Langevin dynamic simulations Chremos et al. showed that for star-shaped polymers, possessing 8 arms, 25 Kuhn segments/arm (i.e.  $M_w^{\text{arm}} = 18$  kg/mol. for PS chains [17]), physisorbed onto a surface under theta- solvent conditions the ratio of the radius of gyration parallel to the surface to its value perpendicular to the surface is larger than 2 [24]. This indicates that that the star-shaped polymer spreads laterally on the surface. The radius of gyration of the star-shaped polymer in this study is  $R_g = 4.5$  nm. In

light of this it now becomes apparent that since  $h_S^{8\text{arm}}=7.8$  nm, the mesolayer film would be composed of approximately two layers of star-shaped molecules. To this end, the immersion of the sample in a good solvent would have the effect of dissolving the chains not adsorbed to the substrate. Such a procedure was performed and ellipsometric measurements revealed that a  $\sim 2$  nm film remained on the substrate. The thickness of this remaining layer is approximately the same as the thickness expected based on the minimum of the effective interface potential for the star-shaped molecule,  $h_{\text{min}}(\text{star})\sim h_S^{8\text{arm}}$ . Our data indicate that the layer in contact with the substrate formed due to the adsorption of the arms driven from the fact that star polymers can gain adsorption energy while, owing to their architecture, the entropic penalty upon adsorption is expected to be low. However, this particular 8-arm system appears to gain free energy by forming a second layer on the adsorbed, wetting, layer.

It is clear from the foregoing that the macroscopic contact angle of star-shaped macromolecules may be nearly an order of magnitude smaller than their linear analogs. Additionally, the line tension of star-shaped polymers may be as much as two orders of magnitude smaller. The precursor layer surrounding the droplets exists only in the case of low molecular linear weight linear chains for entropic reasons; it is a remnant of the adsorbed layer that broke-up into nano-droplets. On the other hand, the analogous adsorbed layer for star-shaped molecule of sufficiently large number of arms ( $f=8$ ), is stable, even after many days of annealing at elevated temperatures. The differences between the wetting behavior of the thin linear PS and the thin 8 arm star-shaped polymer films are schematically depicted in FIG. 1d. These results are consistent with the notion that star-shaped polymers exhibit significant interfacial activity; [13] they suffer a

significantly lower entropic penalty than their linear analogs of the same  $N$  upon adsorption at an interface [11]; the number of segments of a star-shaped molecule in contact with an interface is large compared to linear chains of the same  $N$  [12]. Moreover, the frustrated segmental packing in the bulk is responsible for the decrease in the cohesive energy density of star-shaped molecules, leads to lower surface tensions than their linear chain counterparts of the same  $N$  [14, 15].

## Acknowledgements

This work was supported by the National Science Foundation, Division of Materials Research, Polymers Program 0906425

## References

- [1] C. Fradin *et al.*, *Nature* **403**, 871 (2000).
- [2] D. T. Wasan, and A. D. Nikolov, *Nature* **423**, 156 (2003).
- [3] D. Bonn *et al.*, *Rev. Mod. Phys.* **81**, 739 (2009).
- [4] P. G. de Gennes, F. Brochard-Wyart, and D. Quere, *Capillarity and Wetting Phenomena* (Springer-Verlag New York, Inc., New York, 2004).
- [5] P. Bryk, and L. G. MacDowell, *J. Chem. Phys.* **129**, 9 (2008).
- [6] L. Leger, and J. F. Joanny, *Rep. Prog. Phys.* **55**, 431 (1992).
- [7] M. Muller, and L. G. MacDowell, *J. Phys.-Condes. Matter* **15**, R609 (2003).
- [8] M. Muller *et al.*, *J. Chem. Phys.* **115**, 9960 (2001).
- [9] P. Muller-Buschbaum *et al.*, *Europhys. Lett.* **40**, 655 (1997).
- [10] P. F. Green, and V. Ganesan, *Eur. Phys. J. E* **12**, 449 (2003).
- [11] A. Striolo, and J. M. Prausnitz, *J. Chem. Phys.* **114**, 8565 (2001).
- [12] M. K. Kosmas, *Macromolecules* **23**, 2061 (1990).
- [13] J. F. Joanny, and A. Johner, *J. Phys. II* **6**, 511 (1996).
- [14] V. S. Minnikanti, and L. A. Archer, *Macromolecules* **39**, 7718 (2006).
- [15] Z. Y. Qian *et al.*, *Macromolecules* **41**, 5007 (2008).
- [16] R. Seemann, S. Herminghaus, and K. Jacobs, *Phys. Rev. Lett.* **86**, 5534 (2001).
- [17] M. Rubinstein, and R. H. Colby, *Polymer Physics* (Oxford University Press, New York, 2003).
- [18] E. Glynos *et al.*, *Phys. Rev. Lett.* **106**, 128301 (2011).
- [19] E. Vitt, and K. R. Shull, *Macromolecules* **28**, 6349 (1995).
- [20] V. S. Minnikanti, and L. A. Archer, *J. Chem. Phys.* **123** (2005).
- [21] G. T. Dee, and B. B. Sauer, *J. Colloid Interface Sci.* **152**, 85 (1992).

- [22] I. C. Sanchez, and R. H. Lacombe, J. Phys. Chem. **80**, 2352 (1976).  
[23] C. N. Likos, Phys. Rep.-Rev. Sec. Phys. Lett. **348**, 267 (2001).  
[24] A. Chremos *et al.*, Soft Matter **6**, 1483 (2010).

## Figure legends

**FIG. 1:** (a) AFM micrograph of a  $\sim 13$  nm linear PS film ( $M_w = 5$  kg/mol.) on  $\text{SiO}_x$  annealed at  $160^\circ\text{C}$  for 10 min. (b) is the amplitude signal image of a  $2 \times 2 \text{ }\mu\text{m}^2$  area at the periphery of a polymeric droplet; small nanometer size droplets are observed while at the periphery of the microdroplet a nanometer precursor layer can be seen. (c) AFM image of a  $\sim 13$  nm star PS film ( $f = 8$  arms and  $M_w^{\text{arm}} = 10$  kg/mol.) annealed for 400 min at  $160^\circ\text{C}$ . (d) is the schematic of a dewetted linear PS film (top) and of a star PS film (bottom) on  $\text{SiO}_x$  at room temperature.

**FIG. 2:** (a) AFM cross sections of a scratched/scored  $\sim 30$  nm star PS film (black line) for the as cast film (black line) and for 24 h at  $160^\circ\text{C}$  (red line). The inset shows a 3D AFM image of the sample after 24 h at  $160^\circ\text{C}$ . (b) Film thickness dependence on temperature of the 7.8 nm star-shaped PS mesolayer with a  $T_g \approx 103.2^\circ\text{C}$ .

**FIG. 3:** Contact angle of a macroscopic droplet versus the radius of curvature for the linear PS (black squares) and the star-shaped PS with 8 arms and  $M_w^{\text{arm}} = 10$  kg/mol. (red circles).

## Figures

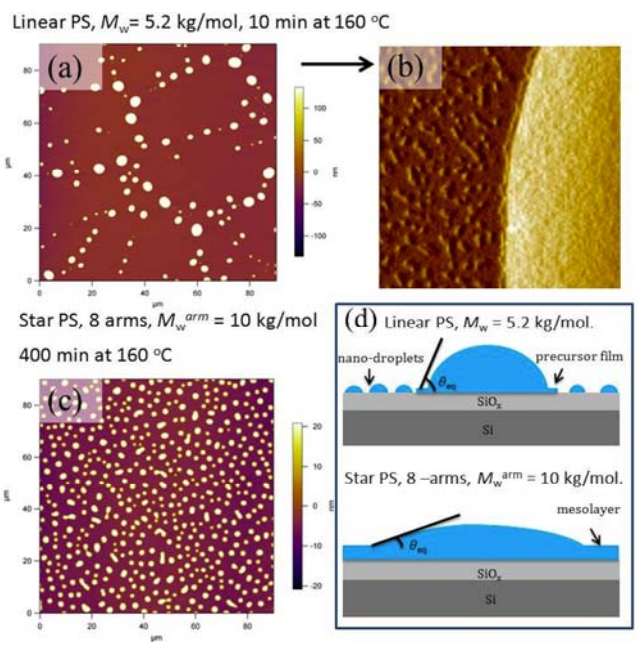


FIG. 1

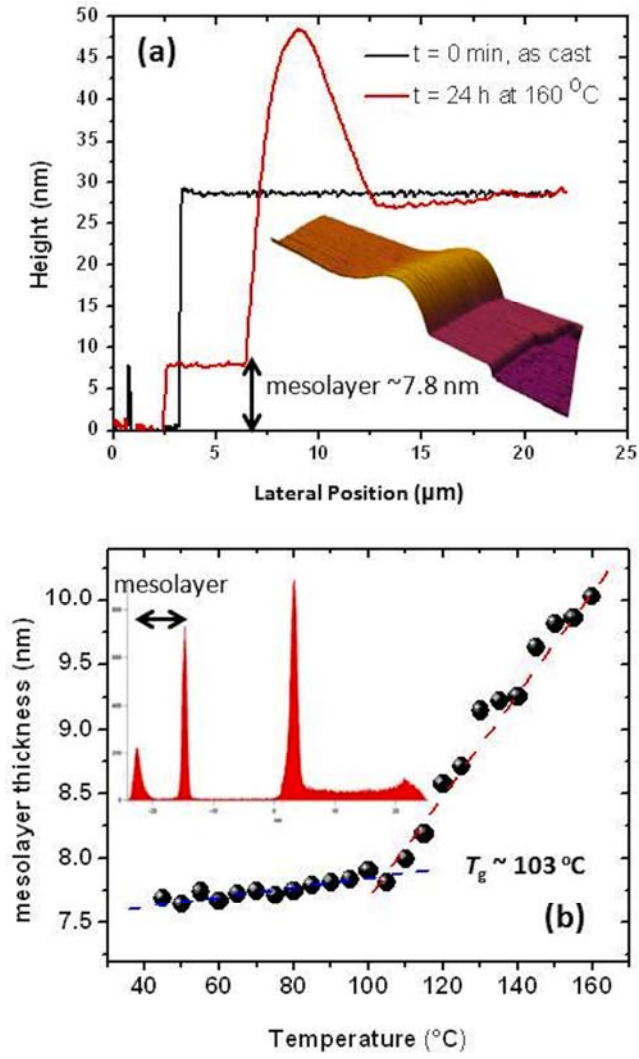
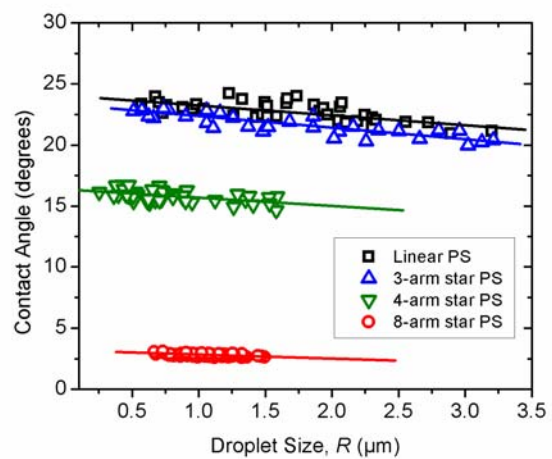


FIG. 2



**FIG. 3**